Comparison of Engineering and CFD Model Predictions for Overpressures in Vented Explosions

Anubhav Sinha, Vendra C. Madhav Rao, Jennifer X. Wen*

Corresponding author: *jennifer.wen@warwick.ac.uk*

School of Engineering, University of Warwick, Coventry, UK.

Abstract

Vented deflagrations are one of the most common and simplest methods to reduce damages that might be caused to buildings and enclosures due to accidental explosions. Various engineering models are available in the literature in the form of published papers, European and USA standards. However, none of these have been sufficiently validated for the vented explosions of hydrogen-air mixtures, especially for realistic explosion scenarios in the presence of obstacles. In addition, a new engineering model based on external cloud explosions (ECE) has been developed by the authors. The foundation of the ECE is the proposed new methodology to calculate the external cloud formation, which is described in another paper (Sinha and Wen, 2018a) also submitted to this conference. The present paper further describes the following up procedures to calculate both the overpressures generated by the external cloud combustion and internal explosion. . The model has also been extended to cover the vented explosions in the presence of obstacles by accounting for the increase in flame surface area due to the presence of obstacles. In parallel to the above, HyFOAM has been developed in house as a dedicated solver for vented hydrogen explosions within the frame of the open source computational fluid dynamics (CFD) code OpenFOAM. The code uses the flame wrinkling combustion model for modelling turbulent deflagrations. Additional sub-models have been added to account for lean combustion properties of hydrogen-air mixtures. In the present study, the overpressure predictions from the various engineering models and the HyFOAM code will be compared with the recently published test data involving hydrogen explosion in a 20-feet ISO container (Skjold et al., 2017a, 2017b).

Keywords: *hydrogen explosions, vented deflagrations, engineering models, external explosion, CFD, HyFOAM.*

1. Introduction

Hydrogen has emerged as a potential "clean fuel" which can replace other gaseous fuels with very little or minimal change in the existing machinery or infrastructure. However there are concerns regarding safety due to the unique combustion characteristics of hydrogen, specifically higher flame speed and enhanced role of flame instabilities. Low strength

buildings and enclosures are generally provided with vent panels which relive pressure in case of accidental explosion. If the vent panel is smaller than the required area, it could be ineffective and result in significant damage to the enclosure. On the other hand, if the vent area is too large, it could result in stronger external explosion which is potentially damaging for nearby installations. So, the vent area and overpressure generated need to be accurately determined in vent panel design. Engineering models (Bauwens et al., 2012a; Molkov and Bragin, 2015) and standards (EN, BS. 14994, 2007; NFPA 68, 2013) are available for predicting the overpressures in vented explosions, however their applicability to hydrogen applications is limited and validation for realistic scenarios is lacking. Numerical modelling is also being developed to simulate the vented explosion processes (Bauwens et. at 2009, Keenan et al 2014). The use of unsteady computational fluid dynamics (CFD) simulations can provide further insight into the underling physics in vented explosions. However, the accuracy of CFD predictions also need to be justified by validations for realistic accidental scenarios (Vendra et. at., 2017a; 2107b).

The present study attempts to address this issue. The objective is to examine the accuracy of pressure predictions from various engineering models and CFD simulations by using a standard experimental study at realistic conditions. Recently, a systematic study was undertaken examining effect of fuel concentration and various model obstacle configurations on overpressure (Skjold et al., 2017a, 2017b). Overpressure measurements from their tests are used in this study to evaluate various EMs and CFD results. Predictions methods are described in brief in section 2. Details on their experimental configuration and operating parameters used are explained in section 3. The new model based on external cloud is described in section 3.5. The results from predictions and their comparison with experimental measurements are given in section 4. The applicability of various prediction methods are also discussed in this section.

2. Engineering Models

The following models are used for this study.

2.1 EN-14994
2.2 NFPA-68
2.3 FM Global model
2.4 Molkov model
2.5 External Cloud model

In the following discussion, each of the above stated model is described briefly, summarising their main features and predicting capabilities.

2.1. EN-14994 (2007) – This model is the statutory standard to be followed for all installations across Europe. This model is based on the concept of gas explosion constant K_G. K_G signifies the maximum rate of pressure rise inside a closed vessel under standard conditions. This model is divided into two formulations, one for a compact enclosure (with $L/D \leq 2$) and the other for elongated enclosure (with $L/D > 2$). The elongated enclosure formulation is applicable for the present study. This formulation does not account for presence of obstacles.

2.2 NFPA (2013) - The National Fire Protection Association's (NFPA) standard on explosion protection by deflagration venting (2013) model considers mixture composition, dimensions of the enclosure and vent area. It recommends considering the worst cases scenario and calculates for the most reactive stoichiometric mixture, unless it is documented and established that stoichiometric mixture cannot form for the enclosure in question. For vent area, it gives different coefficient of discharge based on whether the vent occupies all wall area or is smaller than the wall on that side. Finally, the maximum overpressure is calculated based on an iterative procedure.

2.3 FM Global model (Bauwens et al. (2012)) – This model considers multi-peak nature of overpressure in vented deflagrations, and is the only model to consider multiple peaks. It computed for three peaks- first peak generated by external explosion (P1), second peak is concerned with the oscillatory behaviour of flame giving rise to flame-acoustic interaction (P2). The third peak is seen with cases with obstacles and is denoted as P3. The final peak overpressure is calculated as being the maximum value of these three peaks. This model calculates the maximum flame area in each configuration of ignition location, obstacles, etc. which gives the maximum pressure generated. This model accounts for several physical properties of reactants and products into its formulation. For this study, the values for physical properties are taken from Gaseq calculator (gaseq.co.uk).

2.4 Molkov model – Molkov and Bragin (2015) have developed a vent sizing correlation based on the dependence of overpressure to the turbulent Bradley number. This model does not account for the multi-peak nature of vented deflagrations, but is based on the DOI formulation using the Bradley number for flame exiting through the vented area. Several factors like initial turbulence, aspect ratio of enclosure, turbulence generated by the leading flame front, etc. are taken into account.

More details about these model predictions and comparison with other experimental studies can be found in our previous reports (Sinha, et al., 2017a, 2017b).

2.5. External Cloud Model - The external cloud model accounts for various physical processes occurring in vented explosions and provides a set of equations concerned with each physical step. The vented explosion phenomena can be divided into four major processes:

2.5.1. Ignition and internal flame propagation

2.5.2. Unburnt gas venting and external cloud formation

2.5.3. External explosion

2.5.4. Overpressure generated due to internal burning

2.5.5. Increase in flame surface area due to the presence of obstacles

Now these steps will be explained in detail.

2.5.1. Ignition and internal flame propagation – As the mixture is ignited, the flame front starts growing and finally reaches the vent. For overpressure calculations, the time taken, and flame propagation velocity needs to be calculated. Recent experimental measurements from

Bauwens et al. (2017) have been used to derive the relation for flame velocity and time taken. Flame velocity can be computed using:

$$\frac{U}{U_0} = \left(\frac{R}{R_0}\right)^{\beta} \tag{1}$$

where U is the flame propagation velocity at radius R, U_0 is the flame propagation velocity at R_0, which is the critical radius for the onset of cellular instabilities, and β is fractal excess, experimentally observed to be constant at 0.243 for all hydrogen concentrations (Bauwens et al., 2017). The time taken to reach the vent is computed using this relation:

$$\tau = \left(\frac{R^{(1-\beta)}}{1-\beta}\right)\left(\frac{{R_0}^{\beta}}{U_0}\right) \tag{2}$$

where τ is the time taken by the flame to reach the radial position of R.

2.5.2. Unburnt gas venting and external cloud formation - To study the formation of external cloud, the propagating flame front is assumed to act like a piston, which pushes the unburnt volume through the vent opening in time $\boldsymbol{\tau}$. Further, vortex ring theory given by Sullivan et al. (2008) is used to calculate the cloud radius. First, to calculate the volume of the vented gases forming the cloud, the volume of the flame-ball inside the enclosure is required. The flame-ball is considered to be half ellipsoidal shaped for Back wall ignition. Hence, the burnt volume can be estimated by calculating the volume of the semi-ellipsoid

$$V_b = \frac{\pi}{6} LBH \tag{3}$$

Where L, B and H are the length, breadth and height of the enclosure, respectively. Finally, the volume of cloud can be calculated as:

$$V_c = V_b\left(1 - \frac{1}{\sigma}\right) \tag{4}$$

Now, for the piston, the equivalent radius (R_0) can be calculated by equating the piston surface area to the vent area (A_v)

$$R_0 = \sqrt{\frac{A_v}{\pi}}$$

Piston stroke length using the cloud volume and equivalent piston area:

$$L_P = \frac{V_C}{A_V}$$

Saffman Vortex core size (Sullivan et al., 2008):

$$a = \sqrt{4\,\nu\,\tau}$$

Radius of the vortex ring:

$$R_{Ring} = \sqrt[3]{\frac{3\,R_0^2\,L}{4\alpha}}$$

where, $\alpha = 1$

$$\Lambda = \ln\left(\frac{8R_{Ring}}{a}\right) - B$$

$B = 0.558$, k=0.65, and

$$R_b = \sqrt[3]{\frac{9\,\pi\,R_0^2\,L_P}{4\alpha^2\Lambda\,(1+k)}} \tag{5}$$

Radius of the external cloud is calculated using equation 5. More details about the cloud formation and validation with experimental measurement can be found elsewhere (Sinha and Wen, 2018a). The cloud radius is used to calculate overpressure generated by the external cloud combustion.

2.5.3. External explosion –For external cloud combustion, the flame propagation velocity at cloud radius R_b can be obtained from equation 1. For pressure calculation, assuming Taylor's spherical piston theory (Strehlow, 1981), the Mach number at the cloud radius can be calculated as:

$$M_P = \frac{U_{cloud}}{a_0} \tag{6}$$

and the external pressure generated by this external cloud combustion can be estimated as:

$$P_{ex} = 2\,\gamma_u\left(1 - \frac{1}{\sigma}\right)\sigma^2\,M_P^2 \tag{7}$$

Where γ_u is the ratio of specific heat of unburnt gases, and σ is the expansion ratio. This external pressure will be used for calculating pressure generated inside the enclosure.

2.5.4. Overpressure generated due to internal burning - The fire-ball produced inside the enclosure can be approximated as semi-ellipsoidal, and the flame area can be calculated as:

$$A_f = 2\pi(\sigma - 1)\left(\frac{(ab)^{1.6} + (bc)^{1.6} + (ca)^{1.6}}{3}\right)^{1/1.6} \tag{8}$$

where *a=L, b=B/2,* and *c=H/2*. The flame surface is wrinkled due to Rayleigh-Taylor instability and this wrinkling causes an increase in surface area. Rayleigh-Taylor instability arises when a lighter fluid is accelerated against a heavier fluid. In case of vented deflagrations, lighter burnt gases are accelerating against heavier unburnt gases. The acceleration is caused by the expansion of the burnt gas. Increase in volume of burnt gases due to the expansion will be proportional to (σ-1). It is assumed that the increase in flame

surface area is proportional to and hence it is accounted for in equation 8. The volume of the burnt gases produced, can be calculated as:

$$\dot{V}_b = A_f \, U_f$$

where U_f is the flame propagation velocity calculated by equation 1. Also, the volume of the vented gases can be determined by (Taminini, 1993):

$$\dot{V}_v = u_{cd} \, A_v \sqrt{\frac{p - p_{ex}}{p_{cr} - p_{ex}}} \tag{9}$$

where u_{cd} can be calculated as (Taminini, 1993):

$$u_{cd} = C_d \sqrt{\frac{RT_v}{M_v} \, \gamma \, \frac{\gamma + 1}{2}}$$

where C_d is the coefficient of discharge with constant value of 0.6, R is the universal gas constant, T_v and M_v are the temperature and molecular weight of the vented gases, respectively. They are calculated assuming the vented gases are composed 90% of burnt gases and 10% of unburnt gases. The pressure inside the enclosure is determined by the interplay of two processes. The processes are: (i) pressure increase due to additional volume produced by burning, (ii) decrease in pressure due to venting. At the maximum over-pressure, the volume of the vented gases will be equal to the volume of the burnt gases produced. Hence,

$$A_f \, U_f = u_{cd} \, A_v \sqrt{\frac{p - p_{ex}}{p_{cr} - p_{ex}}} \tag{10}$$

p is the pressure obtained after solving equation 10. It is to be noted that no tuning constants are used in this formulation and the same set of equations are used for all overpressure calculations.

2.5.5. Increase in flame surface area due to the presence of obstacles - Flame propagating past obstacles behave similar to a non-reacting fluid flowing past a bluff body. Flame gets wrapped around these obstacles and at the time of peak internal pressure, there is also a contribution from this wrapped flame surface. The flame surface area around an obstacle sis calculated and is added to the flame surface area in equation 8. The wrapped flame surface area is calculated as:

$$A_{fo} = (\sigma - 1)(P_{obs} + 2 \, L_{recirc}) \; H_{obs} \tag{11}$$

where A_{fo} is the area of wrapped flame around obstacles, P_{obs} is the perimeter of obstacles, is the height of obstacles, and is the L_{rec} length of the recirculation zone, which can be approximated as (Minguez et al., 2011):

$$L_{recirc} = 0.6 \, L_{obs}$$

where L_{obs} is the characteristic length scale of the obstacles, e.g., diameter in case of obstacle with circular cross section. Further details on this external cloud model and validation studies can be found elsewhere (Sinha and Wen, 2018b).

3. CFD modelling – HyFOAM solver

HyFOAM has been developed in-house within the frame of open source Computational Fluid Dynamics (CFD) code OpenFOAM toolbox (OpenFOAM, 2017) for vented lean hydrogen explosions. The fully compressible flow governing equations are solved in explicit Large Eddy Simulation (LES) method. Diffusion terms are discretized using a second-order accurate central differencing scheme and the advective terms approximated using a second-order accurate limited linear scheme. The transient term was discretized using a fully implicit, second-order accurate three-time-level method. A one equation eddy viscosity model is used for evaluating the subgrid scale (SGS) turbulence. The set of governing equations are solved sequentially with iteration over the explicit coupling terms to obtain convergence. The segregate approach results in a Courant number restriction, courant number of 0.1 was used in the numerical simulations.

The Flame Surface Wrinkling Model developed by (Weller et. al.,1998) is adopted for simulating the turbulent deflagrations. This model assumes flame as a very thin interface between the burnt and unburnt gases. A transport equation for flame regress variable (b), where is b =1-c, (c-progress variable) is solved. The combustion model source term variables, flame wrinkle factor (Ξ) and the laminar flame speed (S_L) are updated in the solver development with sub-models to account for the Darrieus-Landau, Rayleigh-Taylor instabilities and Lewis effect in lean turbulent flame speed correlation. The combustion model and the sub-model equations are presented in detail in the accompanying paper in this conference (Vendra et. at 2018) and further in (Vendra et. at 2017a; 2017b).

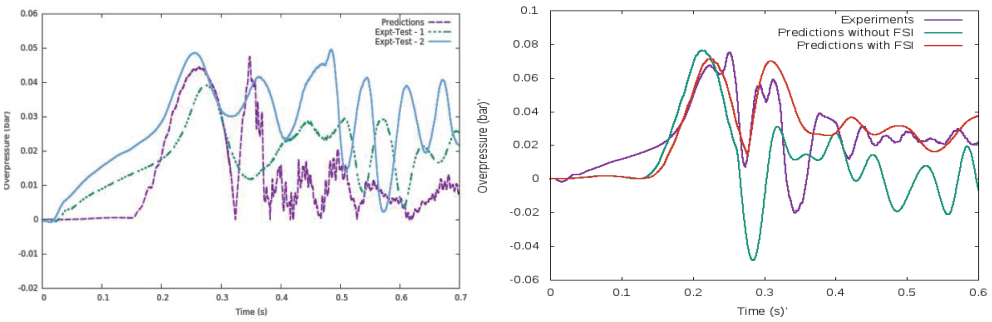

(a) Empty container (b) With bottle basket obstacle

Figure 1. Pressure trace curve at peak overpressure probe location plotted along with experimental measurements for 15% H_2 concentration.

The CFD simulations are performed for the vented lean deflagration in the 20ft ISO container experimental (Skjold et al., 2017a; 2017b) configurations, first to validated against the known experiment test configuration (shown in Table 2) and then carryout the numerical predictions for experimental gap configurations to aid our understanding of the overall overpressure trends with change in H_2 concentration and model obstacles combinations. Figure 1, shows the pressure trace curve at the peak overpressure probe location along with experimental measurements at 15% H_2 concentration levels, for container empty and with bottle basket as obstacle (with back wall center ignition location).

4. Experimental details

The experimental results used for this study have been carried out using standard 20-foot ISO Shipping containers (Skjold et al., 2017a, 2017b). The ISO container is made up of metal sheet 2 mm thick. Corrugations are also provided in container walls to enhance structural rigidity. These containers initially contains atmospheric air, and a specified volume of hydrogen is added to attain the desired equivalence ratio. The mixture is made uniform by mixing through a recirculation system. Spark ignition is provided at the centre of the back wall. Doors of the container, located opposite side to the spark are kept open, providing a venting area of 5.4 m^2. The opening area is initially covered with a thin plastic sheet to contain the hydrogen mixture. This sheet ruptures at a very low pressure, within a small time after the mixture is ignited. In realistic accidental scenarios, the enclosure is likely to contain objects or equipment which will act as obstacles in the flame path, which will affect the flame propagation and peak overpressure. To model these the effects, two different obstacle configuration is used in this study. These configurations used are shown in figure 2- (a) bottle basket and (b) pipe rack.

(a) Bottle basket (b) Pipe rack

Figure 2. Obstacle configurations used in this study (from Skjold et al., 2017a)

4.1 Bottle basket – The bottle basked consists of 20 standard 50 litre cylinders. Each cylinders measured around 1660 mm in length and 230 mm in diameter. These cylinders are held together in a steel frame made up of 50 X 50 mm square pipes. This frame along with the bottles occupies floor area of 1270 mm X 1040 mm. This obstacle configuration is designed to mimic class of solid obstacles that do not allow flame to pass through them and flame usually wraps around the periphery of these obstacles. However, near the top, the bottle neck and valve covers do not cover the total cross sectional area and allow flame to pass through them. They also enhance turbulence and are expected to accelerate the flame.

4.2. Pipe rack – The pipe rack consists of a frame made up of 100 X 100 mm square steel pipes, and circular pipes mounted on this frame. The frame consists of four levels where

circular pipes are mounted. Two types of pipes with diameter 104 mm and 20 mm are used. These pipes are mounted on alternate levels of the frame using U-bolts.

Further details of the experimental facility, obstacle configuration and instrumentation can be found in detailed HySEA report on container tests (Skjold et al., 2017a, 2017b).

4.3 Enclosure wall distortion – This study focusses on low-strength buildings and enclosures, similar to the 20-foot ISO container. For such applications, significant wall distortions are expected for the range of overpressures observed in this study. The enclosure walls distort outward and inward alternately. One such outward distortion is captured in an instantaneous explosion image of this study, shown in figure 3. This oscillatory behaviour is often neglected in literature and is not accounted for in engineering models. However, if these oscillations get coupled with the pressure oscillations, it could lead to higher overpressures. Hence, this behaviour needs to be accounted for in computational studies for accurate calculations. This effect has been incorporated in the present computational studies using pseudo two way coupling between CFD and container structural response (Fluid Structural Interactions-FSI). Details of this FE integration can be found in accompanying paper (Vendra and Wen, 2018).

Figure 3. Wall distortion of 20-foot ISO container during vented explosion as captured in an instantaneous image (from Skjold et al., 2017a)

4.4 Experimental Matrix and obstacle placement- The test matrix using various fuel concentrations and obstacle configurations studied experimentally for the 20-foot ISO container is listed in Table 1 (Skjold et al., 2017a, 2017b). The experimentally measured maximum overpressure is also listed for each case. The cases considered in the present comparative study include the door-vented cases which have a fixed venting area of 5.4 m^2, and the ignition is provided at the wall opposite to the vent area, as shown in Figure 4. The location of both the obstacles inside the container is also shown in Figure 4. Results from the CFD and engineering models are validated with a set of experiments. Further predictions have also been carried out for situations which were experimentally investigated.

The list of the cases studied experimentally for door-venting configuration is shown in Table 1. The list of cases used for validation and predictions is shown in Table 2.

Table 1. Details of cases studied experimentally

Case No	H2%	Configuration	Vent Area (m2)	Ignition location	P-exp (bar)
E1	15	Empty	5.4	BW	*0.042*
E2	15	Bottle Basket (B1)	5.4	BW	*0.062*
E3	18		5.4	BW	0.13
E4	21		5.4	BW	0.19
E5	24		5.4	BW	0.39
E6	15	Pipe Rack (P1)	5.4	BW	0.05
E7	18		5.4	BW	0.12
E8	21		5.4	BW	0.279
E9	21	Pipe + Bottle (P1 B3)	5.4	BW	0.939

(a) Bottle basket

(b) Pipe rack

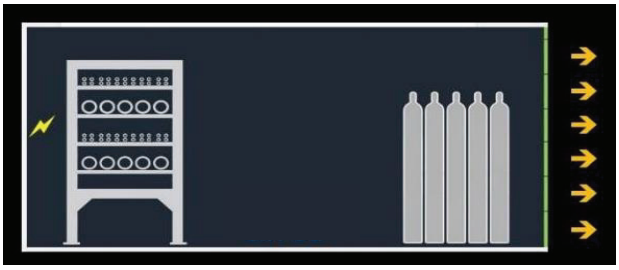

(c) Pipe rack and Bottle Basket

Figure 4. Placement of obstacles inside the 20-feet ISO container. (Skjold, et al. 2017a)

Table 2. Details of cases used for validation and prediction

Case No	H2%	Configuration	Description
E1	15	Empty	Validation
E2	15	Bottle (B1)	
E6	15	Pipe Rack (P1)	
E9	21	Pipe + Bottle (P1 B3)	
P1	18	Empty	Predictions
P2	21	Empty	
P3	24	Empty	
P4	24	Pipe Rack (P1)	
P5	21	Pipe + Bottle (P B)	
P6	21	Pipe + Bottle (P B)	

5. Results and Discussions

Overpressure predictions obtained using the models described in previous sections are compared with the experimental results in Table 3. The results are further shown in Figure 5.

Table 3. Predictions from engineering models and CFD predictions

Case No.	H_2 %	Configuration	P-exp (bar)	EN-14994 (bar)	NFPA-68 (bar)	FM Global (bar)	Molkov (bar)	Ext. Cloud (bar)	CFD (bar)
E1	15	Empty	0.042	0.023	0.028	0.038	0.048	0.03	0.045
E2	15	Bottle (B1)	0.062	0.023	0.028	0.052	0.065	0.04	0.071
E6	15	Pipe Rack (P1)	0.05	0.023	0.028	0.036	0.065	0.04	0.063
E9	21	Pipe + Bottle (P1 B3)	0.939	0.023	0.507	0.786	0.475	0.56	1.211
P1	18	Empty	--	0.023	0.165	0.149	0.088	0.12	0.088
P2	21	Empty	--	0.023	0.507	0.389	0.144	0.35	0.147
P3	24	Empty	--	0.023	1.091	0.761	0.183	0.86	0.659
P4	24	Pipe Rack (P1)	--	0.023	1.091	0.938	0.244	1.12	0.43
P5	21	Pipe + Bottle (P2 B3)	--	0.023	0.507	0.786	0.475	0.56	1.41
P6	21	Pipe + Bottle (B1P2)	--	0.023	0.507	0.786	0.475	0.56	1.30

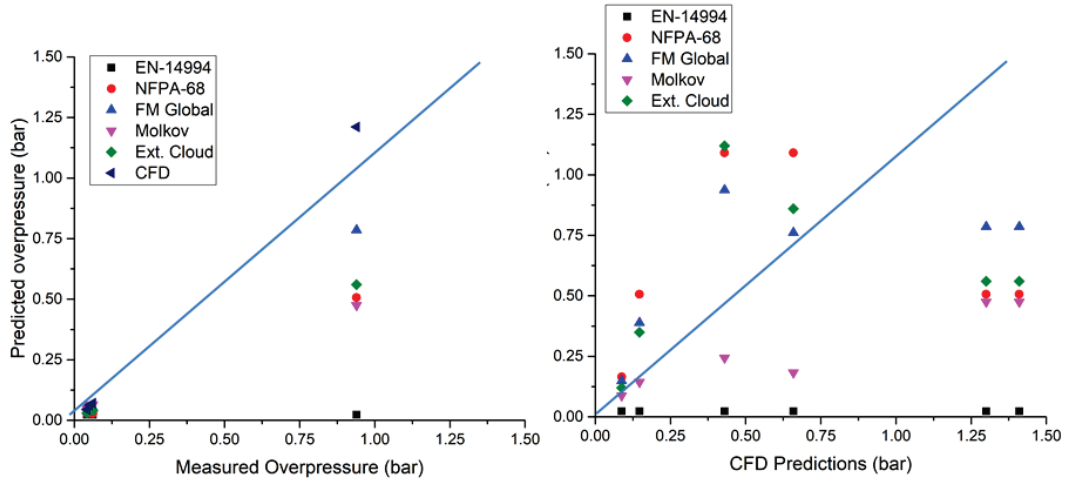

(a) (b)

Figure 5. Comparison of predictions (a) EM and CFD predictions compared with experimental measurements, (b) Cases where experimental results are not available, EM predictions are compared with CFD.

A reasonable match is obtained using NFPA-68, FM Global, Molkov, and the newly developed External cloud models. EN-14994 model considers the worst case scenario and is dependent only on geometry. Hence, same overpressure values are obtained for all cases. It also doesn't account for effect of obstacles, hence significant under-prediction is observed when overpressure increases due to obstacles (see case E6 and E9). Moreover, the Molkov model does consider effects of obstacles but does not specifies formulation to calculate obstacle coefficient Ξ_0. Hence, it is used based on the best-fit with experimental data. Ξ_0 =1.25 is found to give optimum value for both bottle basket and pipe rack. And Ξ_0 =2.5 is used when pipe and bottle both are used together. The uncertainty in estimating Ξ_0 accurately results in under-prediction in Case E9. On the other hand, both the FM Global and the newly developed External cloud model give formulations to account for the effect of obstacles. The same formulation is used for all cases in these models without any additional assumptions or tuning of the constants. Another interesting behaviour is the resulting change in overpressure by changing the location of obstacles, as shown in cases P5 and P6. This effect is not considered in any of the models examined here including the newly developed External cloud model. Work is underway to further improve the new model in this aspect.

6. Conclusions

A comparative study is undertaken for assessing the performance of various engineering models and computational strategies. Engineering models available in the literature and standards are used to obtain overpressure predictions. A new model based on external cloud explosion is also proposed. It is observed that NFPA-68, FM Global, Molkov, and External cloud models give reasonably accurate prediction. Further, CFD predictions are also made

and compared with the experimental results. The validated CFD modelling is able to reproduce the experimental overpressure trends within the limits of the experimental uncertainties.

Acknowledgements

The HySEA project (www.hysea.eu) receives funding from the Fuel Cells and Hydrogen Joint Undertaking under grant agreement No 671461. This Joint Undertaking receives support from the European Union's Horizon 2020 research and innovation programme and United Kingdom, Italy, Belgium and Norway.

References

Bauwens, C. R., Chaffee, J., & Dorofeev, S. B. (2011). Vented explosion overpressures from combustion of hydrogen and hydrocarbon mixtures. *International Journal of Hydrogen Energy*, *36*(3), 2329-2336.

Bauwens, C. R., Chao, J., & Dorofeev, S. B. (2012a). Effect of hydrogen concentration on vented explosion overpressures from lean hydrogen–air deflagrations. *International journal of hydrogen energy*, *37*(22), 17599-17605.

Bauwens, C. R., J. Chao, and S. B. Dorofeev. "Evaluation of a multi peak explosion vent sizing methodology (2012b) In: *IX ISHPMIE. International Symposium on Hazard, Prevention and Mitigation of Industrial Explosions*.

Bauwens, C. R. L., J. M. Bergthorson, and S. B. Dorofeev (2017), Experimental investigation of spherical-flame acceleration in lean hydrogen-air mixtures. *International Journal of Hydrogen Energy* 42.11, pp. 7691-7697.

EN, BS. 14994: 2007. Gas Explosion Venting Protective Systems (2007).

www.gaseq.co.uk

Minguez, M., Brun, C., Pasquetti, R., & Serre, E. (2011). Experimental and high-order LES analysis of the flow in near-wall region of a square cylinder. *International Journal of Heat and Fluid Flow*, 32(3), 558-566.

Molkov, V., Bragin, M. (2015). Hydrogen–air deflagrations: Vent sizing correlation for low-strength equipment and buildings, *International Journal of Hydrogen Energy*, 40(2), 1256-1266.

NFPA 68. (2013): Standard on explosion protection by deflagration venting, 2013.

Bauwens C. R, Chaffee J., Dorofeev S. B., (2009), Experimental and Numerical Study of Methane-air Deflagrations in a Vented Enclosure, *Fire Safety Science*, 9:1043-1054.

Keenan J.J., Makarov D. V., Molkov V. V., (2014), Rayleigh Taylor instability: Modelling and effect on coherent deflagrations, *International Journal of Hydrogen Energy, http://dx.doi.org/10.1016/j.ijhydene.2014.03.230.*

Vendra C. Madhav Rao, Jennifer X. Wen, (2017a) "Numerical Modelling of Vented Lean-Hydrogen-Air Deflagrations using HyFOAM, *26th International Colloquium on the Dynamics of explosion and Reactive Systems*, 30 July-4 Aug, Boston, USA, DOI: 10.5281/zenodo.1134923.

Vendra C. Madhav Rao, Jennifer X. Wen, (2017b) "Vented Hydrogen deflagrations in an ISO Containers, *International Conference on Hydrogen Safety*, 11-13 Sept, Germany. DOI:10.5281/zenodo.1135082.

Vendra C. Madhav Rao, Wen, J.X., (2018), Fluid structure interactions modelling in Vented lean deflagrations, *12th International Symposium on Hazards, Prevention, and Mitigation of Industrial Explosions (ISHPMIE),* Kansas, USA, Aug 2018.

www.openfoam.org , 2017.

Weller, H. G., Tabor, G., Gosman, A. D., and Fureby, C., (1998), Application of a flame wrinkling LES combustion model to a turbulent mixing layer (1998), Proc. of Combust. Inst., 27.

Sinha, A., Vendra. C. Madhav Rao, & Wen, J. X. (2017a). Evaluation of Engineering Models for Vented Lean Hydrogen Deflagrations. In: *27th International Colloquium on the Dynamics of Explosions and Reactive Systems (ICDERS), Boston, USA*

Sinha, A., Vendra C. Madhav Rao, Wen, J. X, (2017b) Performance Evaluation of Empirical Models for Vented Lean Hydrogen Explosions, In *7th International Conference on Hydrogen Safety, Hamburg, Germany*.

Sinha, A., & Wen, J. X, (2018a) Phenomenological Modelling of External Cloud Formation in Vented Explosions, In: *12th International Symposium on Hazards, Prevention, and Mitigation of Industrial Explosions (ISHPMIE),* Kansas, USA, Aug 2018

Sinha, A., & Wen, J. X, (2018b) Performance Evaluation of Empirical Models for Vented Lean Hydrogen Explosions, *International Journal of Hydrogen Energy*, under review.

Sullivan, I. S., Niemela, J. J., Hershberger, R. E., Bolster, D., & Donnelly, R. J. (2008). Dynamics of thin vortex rings. *Journal of Fluid Mechanics*, *609*, 319-347.

Skjold, T., Hisken, H., Lakshmipathy, S., Atanga, G., van Wingerden, M., Olsen, K.L., Holme, M.N., Turøy, N.M., Mykleby, M. & van Wingerden, K. (2017a). Experimental investigation of vented hydrogen deflagrations in containers, Part 1: Homogeneous mixtures, *Report HySEA-D2-04-2017,* July 2017: 304 pp.

Skjold, T., Hisken, H., Lakshmipathy, S., Atanga, G., van Wingerden, M., Olsen, K.L., Holme, M.N., Turøy, N.M., Mykleby, M. & van Wingerden, K. (2017b). Vented

hydrogen deflagrations in containers: effect of congestion for homogeneous mixtures. ICHS-2017.

Strehlow, R.A. (1981) Blast wave from deflagrative explosions: an acoustic approach. *13thAIChE Loss Prevention Symposium*, Philadelphia.

Tamanini, F., (1993), Characterization of mixture reactivity in vented explosion, In: *14th International Colloquium on the Dynamics of Explosions and Reactive Systems*.

This paper appears in the Proceedings of the

Twelfth International Symposium on Hazards, Prevention and Mitigation of Industrial Explosions (XII ISHPMIE)

Edited by Jérôme Taveau and Trygve Skjold

ISBN 978-1-5323-8443-1
90000>
9 781532 384431

Published by Fike Corporation, Blue Springs, MO, USA

The editors compiled the proceedings (1210 pp.) from the files submitted by the authors.

Fike Corporation organized XII ISHPMIE at the Westin Crown Center,
1 East Pershing Road, Kansas City, MO 64108, USA
on 12-17 August 2018

XII ISHPMIE
Kansas City, MO August 12–17, 2018